NASA
Technical
Paper
2518

October 1985

A Method for Determining Acoustic-Liner Admittance in Ducts With Sheared Flow in Two Cross-Sectional Directions

Willie R. Watson

NASA

NASA Technical Paper 2518

1985

A Method for Determining Acoustic-Liner Admittance in Ducts With Sheared Flow in Two Cross-Sectional Directions

Willie R. Watson

Langley Research Center
Hampton, Virginia

NASA
National Aeronautics and Space Administration

Scientific and Technical Information Branch

SYMBOLS

$[A]$ stiffness matrices for discretized finite-element region

$[\bar{A}],[\bar{B}]$ upper triangular matrices

$[A^q],[B^q]$ element stiffness and mass matrix, respectively, for element q

a width of rectangular element

$a_{I,J'}, \bar{a}_{I,J'}, b_{I,J}, \bar{b}_{I,J}$ complex matrix coefficients

$[B]$ mass matrices for discretized finite-element region

b height of rectangular element

c ambient speed of sound

E residual error

F acoustic pressure function for impedance tube

F_ℓ, M_ℓ respective value of pressure eigenfunction and mean-flow profile at node ℓ

f_1, f_2 one-dimensional shape functions

H,L height and width, respectively, of impedance tube

K free-space wave number

K_x dimensional axial propagation constant

$\tilde{K}_x$ dimensionless axial propagation constant

ℓ node number

M mean-flow profile

M_o centerline Mach number

m cross-mode order

n integer 1 or 2 denoting particle velocity or particle displacement, respectively

NY,NZ total number of elements in y- and z-direction, respectively

N_ℓ two-dimensional shape function

SPL sound pressure level

P acoustic pressure

t time

x,y,z Cartesian coordinates

x_I, y_I, z_I Cartesian coordinate values at node I

$\beta_1, \beta_2, \beta_3, \beta_4$ acoustic admittances of wall lining

$\bar{\beta}_m$ acoustic admittance

η, ξ dimensionless local coordinate system for element

λ_m eigenvalue for cross-mode order, m

$\{\phi\}$ global vector of unknowns

$\{\phi^q\}$ vector of unknown nodal values for element q

ω angular frequency

Subscripts:

I,J,m integers

Superscript:

tr vector transpose

Mathematical notation:

[ ] matrix

{ } vector

det | | determinate of matrix

INTRODUCTION

The reduction of high intensity noise radiating from jet engine aircraft has been the subject of continuous investigation for the past two decades. At the present time, mathematical models for predicting the noise radiated from these engines are well developed (ref. 1). However, these prediction models cannot be used with confidence to predict noise levels radiating from a jet engine in a realistic flow environment. Before this confidence can be achieved, it is necessary to obtain accurate determinations of the physical parameters, which are input to the prediction models. The two critical input parameters are the source input and the admittance of the sound-absorbing material. This paper addresses the determination of the latter of these two important input parameters.

Experiments with sound-absorbing materials in the presence of flow indicate significant differences in acoustic performance as the mean-flow Mach number is varied (ref. 2). This necessitates that sound-absorbing properties of acoustic materials be evaluated experimentally in flow. To account for the effects of the mean flow, a test sample of the acoustic-lining material is normally installed in a grazing-flow impedance tube with a controlled aeroacoustic environment. In such a grazing-flow impedance tube, usually rectangular in cross section, the acoustic material is aligned so that the sound and mean-flow graze over its surface in a manner simulating an engine environment. In principle, the acoustic admittance can be determined by direct measurements of normal particle velocity and pressure since acoustic admittance is the ratio of normal particle velocity to pressure at the wall surface. However, measurements of normal velocity in the presence of grazing flow are not reliable. Instead, an indirect measurement approach (ref. 3) has been used which makes use of changes in the wave field caused by the introduction of the test sample in the hard-walled impedance tube. These measurements are then used to calculate the acoustic admittance.

Analytical methods for directly determining acoustic admittances from pressure measurements taken in a grazing-flow impedance tube have progressed slowly. Armstrong, Beckemeyer, and Olsen (ref. 2) developed a method that is restricted to thin boundary-layer flows with shear in one cross-sectional direction of the tube. This method used an asymptotic expansion to derive a boundary condition that is applicable at the boundaries of the uniform region in which an exact solution is possible. Mungur and Gladwell (ref. 3) developed a method that is applicable to more general boundary layers, including cases where the boundary layer spans the entire tube. This method is based upon a Runge-Kutta integration across the boundary layer and is restricted to grazing flows with shear in a single cross-sectional direction. Watson (ref. 4) developed a finite-element method for calculating acoustic admittances from acoustic pressure data in a grazing-flow impedance tube with one-dimensional shear.

The methods presented in references 2, 3, and 4 are restricted to infinitely long test samples with mean shear in a single cross-sectional direction of an impedance tube. However, grazing-flow duct facilities commonly employ ducts with a relatively small rectangular cross section in which the grazing flow possesses shear in both cross-sectional directions of the impedance tube, such as the flow impedance test laboratory at the Langley Research Center. Thus, the present effort was moti-

vated by the need to account for the more realistic flow environment with shear in both cross-sectional directions of laboratory flow-impedance tubes.

This paper describes a method for determining the admittance of an acoustic material in a grazing-flow impedance tube in which the grazing flow is assumed to possess shear in both cross-sectional directions. The analysis is restricted to sound fields which are dominated by a single propagating mode. The method is developed explicitly for rectangular ducts, although the approach is applicable to other duct geometries as well. Experimental input data needed include an estimate of the axial propagation constant, the two-dimensional mean-flow profile, and acoustic pressures parallel to the treated wall of the impedance tube. From these experimentally determined characteristics of the aeroacoustic field, the admittance can be calculated. In this paper, the unknown admittance value is obtained by solving an eigenvalue problem. This eigenvalue problem results from the application of the finite-element method to the partial differential equation and boundary conditions governing the acoustic field.

The paper is divided into four sections. The first section presents the governing partial differential equation and boundary conditions. In the second section, a finite-element scheme is applied to obtain the solution to this problem. The finite-element method leads to an eigenvalue problem which requires a special scheme to obtain its solution. This eigenvalue solution scheme is developed in the third section of this paper. Finally, the paper closes with a discussion of some applications.

MATHEMATICAL FORMULATION

Figure 1 depicts the cross-sectional geometry of the grazing-flow impedance-tube test section and its coordinate system. All four walls of the tube are lined with acoustic treatment and are assumed infinite in extent. The mathematical development assumes that the mean flow in the test section is axial and fully developed, so that flow gradients exist only in the y- and z-direction.

The solution of the wave equation for harmonic time dependence in the presence of shear can be written in the form:

$$P(x,y,z,t) = F(y,z)e^{-i(K_x x-\omega t)} \tag{1}$$

where K_x is the axial propagation constant. The following elliptic partial differential equation for the pressure function $F(y,z)$ is obtained (ref. 5):

$$E(y,z) = (1 - M\tilde{K}_x)[F_{yy} + F_{zz}] + 2\tilde{K}_x[M_y F_y + M_z F_z]$$

$$+ K^2[(1 - M\tilde{K}_x)^3 - \tilde{K}_x^2(1 - M\tilde{K}_x)]F = 0 \tag{2}$$

where

$$\tilde{K}_x = \frac{K_x}{K}$$

In equation (2), the function $M = M(y,z)$ is the mean flow profile, $\tilde{K}_x$ is the dimensionless axial propagation constant in the impedance tube, and K is the free-space wave number (ω/c).

The physical boundary conditions associated with equation (2) require either continuity of particle displacement or continuity of normal particle velocity along the four walls of the impedance tube (ref. 1). These boundary conditions can be expressed in the form:

$$F_z(y,0) = -iK\beta_1\left[1 - M(y,0)\tilde{K}_x\right]^n F(y,0) \tag{3}$$

$$F_z(y,L) = iK\beta_2\left[1 - M(y,L)\tilde{K}_x\right]^n F(y,L) \tag{4}$$

$$F_y(0,z) = -iK\beta_3\left[1 - M(0,z)\tilde{K}_x\right]^n F(0,z) \tag{5}$$

$$F_y(H,z) = iK\beta_4\left[1 - M(H,z)\tilde{K}_x\right]^n F(H,z) \tag{6}$$

where β_1, β_2, β_3, and β_4 are the specific acoustic admittances of the acoustically lined walls. (See fig. 1.) Continuity of acoustic particle displacement at the lined walls are obtained by setting the integer n to 2, whereas continuity of acoustic particle velocity is obtained by setting n to 1. It is instructive to note that realistic mean-flow profiles satisfy the condition of no slip at the boundaries rendering a zero mean flow there. Thus, for realistic mean flows, both forms of the boundary condition coalesce to the same expression at each wall. However, since some unrealistic mean velocity profiles are used in this paper in order to check with former works, n will be carried throughout the analysis as a parameter.

Equations (2) through (6) constitute a boundary value problem for the acoustic pressure function $F(y,z)$. The axial propagation constant $\tilde{K}_x$, free-space wave number K, mean-flow profile $M(y,z)$, boundary condition order n, and wall-lining admittances β_1, β_2, and β_3 are assumed specified and are treated as known. The homogeneity of equations (2) through (6) then allows the determination of the function $F(y,z)$ and unknown acoustic admittance β_4.

Upon obtaining the value of the necessary parameters, the boundary value problem posed by equations (2) through (6) can be solved to obtain the function $F(y,z)$ and unknown admittance β_4. However, equation (2) is a partial differential equation with variable coefficients and its solution can be put in terms of known functions only for some special cases of the two-dimensional sheared flow, $M(y,z)$. However, these cases cannot generally be achieved in the laboratory and are not useful for general application. Thus, the admittance and pressure eigenfunction $F(y,z)$ must

be determined numerically for mean flows of practical interest. A numerical method for finding these solutions is described in the following section.

NUMERICAL SOLUTION TECHNIQUE

Two principal decisions in the adoption of a numerical technique were the use of a Galerkin finite-element method and use of linear shape functions to approximate the pressure function and mean-flow profile. The discretization mesh is shown in figure 2. The cross-sectional area of the impedance tube has been divided into NY and NZ elements in the y- and z-direction, respectively. A typical element (I,J) has length $(z_{I+1} - z_I)$ and $(y_{J+1} - y_J)$ in the z- and y-direction, respectively. In order to generalize and also simplify the formulation, it is convenient to define a local coordinate system for each element. This local coordinate system, shown in figure 3, also facilitates the integration which is required to obtain the element equation.

In order to develop the element equations for a typical element (I,J), the pressure function $F(\eta,\xi)$ and mean-flow profile $M(\eta,\xi)$ are expressed in a form which ensures continuity of these functions both within the element and also along lines which are common between any two of the elements. In a typical element, these functions are approximated by linear interpolation functions of the form

$$F(\eta,\xi) = N_\ell(\eta,\xi)\, F_\ell \qquad (\ell = 1 \text{ to } 4) \tag{7}$$

$$M(\eta,\xi) = N_\ell(\eta,\xi)\, M_\ell \qquad (\ell = 1 \text{ to } 4) \tag{8}$$

in which repeated subscripts are to be summed over, F_ℓ and M_ℓ are the values of the functions $F(\eta,\xi)$ and $M(\eta,\xi)$ at node ℓ of the element, and

$$N_1 = f_1(\eta,b)\, f_1(\xi,a) \tag{9}$$

$$N_2 = f_1(\eta,b)\, f_2(\xi,a) \tag{10}$$

$$N_3 = f_2(\eta,b)\, f_2(\xi,a) \tag{11}$$

$$N_4 = f_2(\eta,b)\, f_1(\xi,a) \tag{12}$$

$$f_1(\eta,b) = 1 - \frac{\eta}{b} \tag{13}$$

$$f_2(\eta,b) = \frac{\eta}{b} \tag{14}$$

In applying the Galerkin version of the method of weighted residuals, the residual error $E(\eta,\xi)$ in each element is multiplied by the basis function $N_\ell(\eta,\xi)$ and integrated over the element to obtain

$$\int_0^a \int_0^a E(\eta,\xi)\, N_\ell(\eta,\xi)\, d\eta\, d\xi$$

This integral expresses the desired averaging of the residual error but it does not admit the influence of the wall boundary conditions. Integration by parts is now incorporated to reduce the order of the second derivative terms in this integration and to incorporate the boundary conditions:

$$\begin{aligned}
\int_0^a \int_0^b E(\eta,\xi)\, N_\ell(\eta,\xi)\, d\eta\, d\xi = -\Bigg\{ \int_0^a \int_0^b \Bigg[& \frac{\partial F}{\partial \eta}\frac{\partial N_\ell}{\partial \eta} + \frac{\partial F}{\partial \xi}\frac{\partial N_\ell}{\partial \xi} - \tilde{K}_x M\left(\frac{\partial F}{\partial \eta}\frac{\partial N_\ell}{\partial \eta}\right. \\
& \left. + \frac{\partial F}{\partial \xi}\frac{\partial N_\ell}{\partial \xi}\right) - 3\tilde{K}_x\left(\frac{\partial M}{\partial \eta}\frac{\partial F}{\partial \eta} N_\ell\right) + \frac{\partial M}{\partial \xi}\frac{\partial F}{\partial \xi} N_\ell \\
& + K^2\left(3K_x - \tilde{K}_x^3\right) MFN_\ell + K^2\left(\tilde{K}_x^2 - 1\right) FN_\ell \\
& - 3K^2\tilde{K}_x^2 MFN_\ell + K^2\tilde{K}_x^3 M^3 FN_\ell \Bigg]\, d\eta\, d\xi \Bigg\} \\
& + \int_0^a \Bigg\{ \left[1 - \tilde{K}_x M(b,\xi)\right] \frac{\partial F}{\partial \eta}(b,\xi)\, N_\ell(b,z) \\
& - \left[1 - \tilde{K}_x M(0,\xi)\right] \frac{\partial F}{\partial \eta}(0,\xi)\, N_\ell(0,\xi) \Bigg\}\, d\xi \\
& + \int_0^b \Bigg\{ \left[1 - \tilde{K}_x M(\eta,a)\right] \frac{\partial F}{\partial \xi}(\eta,a)\, N_\ell(\eta,a) \\
& - \left[1 - \tilde{K}_x M(\eta,0)\right] \frac{\partial F}{\partial \xi}(\eta,0)\, N_\ell(\eta,0) \Bigg\}\, d\eta
\end{aligned} \tag{15}$$

Boundary conditions are now incorporated at the element level by replacing the normal derivative of the function F along the outer boundaries of the discretized region by its value from the boundary conditions. For example, $\frac{\partial F}{\partial \eta}(b,\xi)$ along the boundary $y = H$ is replaced by $iK\beta_4[1 - M(b,\xi)K_x]^n F(b,\xi)$. This procedure is standard practice in finite-element methodology since it avoids the difficult task of having to choose basis functions which satisfy the boundary conditions. Substituting equations (7) through (14) into equation (15) gives

$$\int_0^b \int_0^a E(\eta,\xi)\, N_\ell(\eta,\xi)\, d\xi\, d\eta = [A^q]\{\phi^q\} + \beta_4[B^q]\{\phi^q\} \tag{16}$$

in which $[A^q]$ and $[B^q]$ are the stiffness and mass matrix for the element, β_4 is the unknown admittance value, and $\{\phi^q\}$ is a vector containing the unknown values of the function $F(\eta,\xi)$ at the four nodes of the element.

Assembly of a global matrix equation representing the discretized region (fig. 2) from a set of finite-element matrix equations is a basic procedure in the finite-element technique. Appropriate shifting of rows and columns are all that is required to add the local element matrix directly into the global matrix (ref. 6). The result is a set of linear matrix equations which is expressible in the form:

$$[A]\{\phi\} = \beta_4[B]\{\phi\} \tag{17}$$

The global matrices $[A]$ and $[B]$ are both square matrices whose order is $(NY + 1)(NZ + 1)$ and $\{\phi\}$ is a vector consisting of the values of $F(\eta,\xi)$ at the various nodes of the system.

Equation (17) has the form of a generalized eigenvalue problem. Here, the unknown admittance β_4 is the eigenvalue and is determined by the determinant condition

$$\det\left|[A] - \beta_4[B]\right| = 0 \tag{18}$$

Equation (18) is the basic equation which must be solved to obtain the unknown admittance β_4.

Some further comments concerning equation (18) should be made in order to avoid some confusion. First, there are many values of β_4 which satisfy equation (18) and this appears to be at odds with the physical problem for which only a single value of the admittance β_4 exist. Secondly, equation (18) must be solved with an eigenvalue extraction algorithm on a digital computer. In this paper, the LZ algorithm (ref. 7) is employed on a Control Data 6600 computer system to exact the solution to equation (18). The order of the coefficient matrices $[A]$ and $[B]$ was restricted to 100 when the algorithm was employed on this machine. This restriction is due to the core limitation of the central memory of the computer and is equivalent to a maximum

of nine elements in both the y- and z-directions of the impedance tube. Since 10 elements per wavelength are needed to resolve the acoustic wave, this would restrict the analysis to only plane waves, a situation which rarely exists physically.

In the following section, a determinate search routine is developed which takes advantage of the character of the coefficient matrices in equation (18) and increases the maximum number of points in the y- and z-direction of the impedance tube by more than an order of magnitude. It is also shown how to extract the correct value of the unknown admittance β_4 from the many values which are obtained from the solution to equation (18).

DETERMINATE SEARCH TECHNIQUE

Generalized eigenvalue problems for large systems such as equation (17) are solved by numerical schemes that are either direct or iterative. With the improvement in digital computer hardware, direct methods have proved to be more versatile and reliable and are used in this paper. In the direct approach, both [A] and [B] are transformed to upper triangular form and the solution to the transformed system is obtained directly. Fortunately, in the finite-element application, the equations are amendable to direct solution techniques that take advantage of the special character of [A] and [B]. The general form for the coefficient matrices [A] and [B] are as follows:

$$[A] = \begin{bmatrix} a_{1,1} & a_{1,2} & & & & & \\ a_{2,1} & a_{2,2} & a_{2,3} & & & & \\ & a_{3,2} & a_{3,3} & a_{3,4} & & & \\ & & \cdot & \cdot & \cdot & & \\ & & & \cdot & \cdot & \cdot & \\ & & & & a_{NY+1,NY} & a_{NY+1,NY+1} \end{bmatrix} \tag{19}$$

$$[B] = \begin{bmatrix} 0 & 0 & & & & \\ 0 & 0 & 0 & & & \\ & 0 & 0 & 0 & & \\ & & \cdot & \cdot & \cdot & \\ & & & \cdot & \cdot & \cdot \\ & & & & 0 & b_{NY+1,NY+1} \end{bmatrix} \tag{20}$$

While the unknown vector $\{\phi\}$ is partitioned in the form (eq. (17)):

$$\{\phi\}^{tr} = \{\phi_1, \phi_2, \phi_3, \ldots, \phi_{NY}, \phi_{NY+1}\} \tag{21}$$

In equations (19) through (21) the submatrices $a_{I,J}$ and $b_{NY+1,NY+1}$ are square matrices whose orders are (NZ + 1), and $\{\phi_I\}$ are column vectors of the same order. Further, the submatrices $a_{I,J}$ and $b_{NY+1,NY+1}$ are tridiagonal. Thus, [A] is a block tridiagonal matrix and [B] has a single nonzero tridiagonal block in its last row and column.

Because of the character of the coefficient matrices [A] and [B], equation (17) is fairly easy to solve. There are three steps that are executed recursively:

1. Use fully pivoted row operations to reduce [A] to block upper triangular form, executing the same row operations on the matrix [B]. The resulting generalized eigenvalue problem will be of the form:

$$[\bar{A}]\{\phi\} = \beta_4[\bar{B}]\{\phi\} \tag{22}$$

$$[\bar{A}] = \begin{bmatrix} \bar{a}_{1,1} & \bar{a}_{1,2} & & & & & \\ & \bar{a}_{2,2} & \bar{a}_{2,3} & & & & \\ & & \bar{a}_{3,3} & \bar{a}_{3,4} & & & \\ & & & \cdot & \cdot & & \\ & & & & \cdot & \cdot & \\ & & & & & \bar{a}_{NY,NY} & \bar{a}_{NY,NY+1} \\ & & & & & & \bar{a}_{NY+1,NY+1} \end{bmatrix} \tag{23}$$

$$[\bar{B}] = \begin{bmatrix} 0 & 0 & & & & & \\ & 0 & 0 & & & & \\ & & 0 & 0 & & & \\ & & & \cdot & \cdot & & \\ & & & & \cdot & \cdot & \\ & & & & & 0 & \bar{b}_{NY,NY+1} \\ & & & & & & \bar{b}_{NY+1,NY+1} \end{bmatrix} \tag{24}$$

2. The eigenvalue β_4 is now extracted from the last equation of this reduced system (eq. (22)):

$$[\bar{a}_{NY+1,NY+1}]\{\phi_{NY+1}\} = \beta_4[\bar{b}_{NY+1,NY+1}]\{\phi_{NY+1}\} \tag{25}$$

Equation (25) is solved by using the LZ algorithm (ref. 7) to obtain β_4 and $\{\phi_{NY+1}\}$. The remaining unknowns, $\{\phi_{NY}\}$, $\{\phi_{NY-1}\}$, ..., $\{\phi_1\}$ are obtained by back substitution:

$$[\bar{a}_{NY,NY}]\{\phi_{NY}\} = [\beta_4\bar{b}_{NY,NY+1} - \bar{a}_{NY,NY+1}]\{\phi_{NY+1}\} \tag{26}$$

$$[\bar{a}_{I-1,I-1}]\{\phi_{I-1}\} = -[\bar{a}_{I-1,I}]\{\phi_I\} \qquad (I = NY,\ NY - 1,\ \ldots,\ 2) \tag{27}$$

3. Matrices [A] and $[\bar{A}]$ are written to mass storage in rectangular form and the nonzero blocks in [B] and $[\bar{B}]$ are stored into the zero blocks of [A] and $[\bar{A}]$:

$$[A] = \begin{bmatrix} 0 & a_{1,1} & a_{1,2} \\ a_{2,1} & a_{2,2} & a_{2,3} \\ a_{3,2} & a_{3,3} & a_{3,4} \\ \cdot & \cdot & \cdot \\ \cdot & \cdot & \cdot \\ a_{NY,NY-1} & a_{NY,NY} & a_{NY,NY+1} \\ a_{NY+1,NY} & a_{NY+1,NY+1} & b_{NY+1,NY+1} \end{bmatrix} \tag{28}$$

$$[\bar{A}] = \begin{bmatrix} \bar{b}_{NY,NY+1} & \bar{a}_{1,1} & \bar{a}_{1,2} \\ \bar{a}_{2,1} & \bar{a}_{2,2} & \bar{a}_{2,3} \\ \bar{a}_{3,1} & \bar{a}_{3,3} & \bar{a}_{3,4} \\ \cdot & \cdot & \cdot \\ \cdot & \cdot & \cdot \\ \bar{a}_{NY,NY-1} & \bar{a}_{NY,NY} & \bar{a}_{NY,NY+1} \\ \bar{a}_{NY,NY} & \bar{a}_{NY+1,NY+1} & \bar{b}_{NY+1,NY+1} \end{bmatrix} \tag{29}$$

The advantage of the technique employed herein is

1. The [B] matrix need not be stored.

2. Only enough space for three columns of the [A] matrix is needed in mass storage.

3. The number of points in the z-direction of the impedance tube which the scheme can now handle is approximately 100 instead of 10, and the number of points in the y-direction of the tube is unlimited.

It should be noted that the solution to equation (25) gives the admittance β_4 and unknown vector $\{\phi_{NY+1}\}$. However, the vector $\{\phi_{NY+1}\}$ only contains values of the function $F(y,z)$ at nodes along the upper wall of the discretized region (fig. 2). To obtain values of the function $F(y,z)$ at points away from the upper wall, equations (26) and (27) must be solved. The thrust of this paper is to determine the unknown admittance β_4; therefore, only equation (25) need be solved.

Some further discussion on the solution to equation (25) is helpful. As mentioned earlier, there are many values of β_4 which satisfy this equation. In fact, there are (NZ + 1) values of β_4 which satisfy this equation, and there will be in general a different eigenfunction $\{\phi_{NY+1}\}$ for each β_4. This result is not surprising since equation (2) is elliptic in character and the boundary condition along the upper wall, $y = H$, was not specified (i.e., the boundary condition was not specified along a closed contour). In short, the discrete set of wall admittances obtained from the solution to equation (25) simply reflect the fact that a unique solution to equations (2) through (6) cannot be obtained unless additional boundary information is given along the upper wall. The solution to equation (25) gives all possible combinations of the upper wall eigenfunctions $\{\phi_{NY+1}\}$ and wall admittance values which can satisfy the boundary condition in equation (6). Suppose a measurement of the upper wall eigenfunction $\{\phi_{NY+1}\}$ is made in the impedance tube. Then this measured upper wall eigenfunction will correspond to one of the solutions for $\{\phi_{NY+1}\}$ obtained from solving equation (25). The admittance β_4 corresponding to this eigenfunction is the correct one ror the problem. This approach will be used in this paper.

RESULTS AND DISCUSSION

In order to verify the numerical technique, results from the method are compared both with exact solutions that can be obtained for a uniform mean-flow profile and with results of reference 4 for cases involving shear in the y-direction only. Next, results are presented for some cases in which the flow possesses shear in both the y- and z-direction of the tube. Results are restricted to a square duct for which $H = L = 1$ foot, $K = 1$ (radians per foot), with 50 elements in the y- and z-directions of the tube ($NY = NZ = 50$). Further, continuity of particle velocity is employed as the boundary condition and the bottom and side walls of the tube are considered rigid ($\beta_1 = \beta_2 = \beta_3 = 0.0 + 0.0i$). The choice of this particular combination of parameters was felt to be sufficient to obtain confidence in the numerical technique.

Uniform Flow

The fundamental equations governing the acoustic pressure eigenfunction (eqs. (2) through (6)) can be solved analytically under the assumption of uniform mean flow. This expression for the eigenfunction is expressed in the following form:

$$F(y,z) = F_m(y) \cos \frac{m\pi z}{L} \qquad (m = 0, 1, 2, \ldots, \infty) \tag{30}$$

$$F_m(y) = \frac{\cos \lambda_m y}{\cos \lambda_m H} \tag{31}$$

where the eigenvalue λ_m is related to the axial wave number by the equation:

$$\lambda_m^2 = K^2\left[\left(M^2 - 1\right)\tilde{K}_x^2 - 2M\tilde{K}_x + \left(1 - \frac{m^2\pi^2}{K^2L^2}\right)\right] \tag{32}$$

Equations (30) through (32) are easily derived by finding the general solution to equations (2) through (5) for a constant M by separation of variables. Note that equation (30) satisfies equations (3) through (5) for rigid boundaries (i.e., $\beta_1 = \beta_2 = \beta_3 = 0.0 + 0.0i$). A generalization of this solution to include nonrigid boundaries is also possible (ref. 1). Equation (30) is incomplete by virtue of the fact that it does not satisfy the upper wall boundary condition. (See eq. (6).) The substitution of equation (30) into equation (6) gives the following equation:

$$\beta_4 = \frac{-\lambda_m \tan (\lambda_m H)}{iK(1 - M\tilde{K}_x)^n} \tag{33}$$

Generally, H, L, K, M, m, n, and β_4 are specified. The objective is then to find the discrete set of axial propagation constants which satisfy equation (33). A single infinity of these axial propagation constants can be found. In this paper, we want to consider the inverse problem. Thus, we wish to specify H, L, K, M, n, and $\tilde{K}_x$; then it is a simple matter to calculate the corresponding values of β_4 from equation (33). There will be a single infinity of these values, one for each value of m, so that

$$\beta_4 = \{\bar{\beta}_0, \bar{\beta}_1, \bar{\beta}_2, \ldots\} \tag{34}$$

$$\bar{\beta}_m = \frac{-\lambda_m \tan(\lambda_m H)}{iK(1 - M\tilde{K}_x)^n} \tag{35}$$

Note that for the problem considered here, a unique value of β_4 is not defined until a prescription is given for singling out a single value for the integer m. The prescription employed is to specify the functional form of the eigenfunction F(y,z) along the upper wall. Evaluating equation (30) along the upper walls gives

$$F(H,z) = \cos \frac{m\pi z}{L} \qquad (m = 0, 1, 2, \ldots, \infty) \tag{36}$$

Thus, a specification of F(H,z) is equivalent to specifying a single value of m.

The major thrust of the numerical method employed here is embodied in the solution to equation (25). The solution to equation (25) gives the discrete set of admittance values specified in equation (34). Further, $\{\phi_{NY+1}\}$ is the solution for F(H,z). If the numerical method has been applied properly, each of the upper wall eigenfunctions $\{\phi_{NY+1}\}$ computed from equation (25) will be of the form $\cos m\pi z/L$, just as in equation (36). In the rest of this section, these ideas will be confirmed with numerical results.

Consider first the solution to equation (35) for $\tilde{K}_x = 2.97819i$ and zero flow (M = 0). In this case, considerable insight into the integrity of the numerical scheme can be obtained since the solution to equation (35) gives $\bar{\beta}_m = 0 + 0i$ for $m < 2$, and $\bar{\beta}_m$ purely imaginary for $m \geq 2$. Although this particular case has no relevance to physical reality, it does test the ability of the numerical method to extract both zero and multiple roots simultaneously. Results are presented in table I, starting at m = 0 and terminating at m = 5. Excellent comparison between the exact admittance values and those extracted by the finite-element method are obtained. The wall pressure eigenfunction F(H,z) is plotted against the exact value for m = 0, m = 1, and m = 2 in figures 4(a), (b), and (c), respectively. The wall pressure eigenfunctions computed from this analysis are undistinguishable from the exact values.

Table II presents results for $\tilde{K}_x = 0.5 + 0.5i$ and zero flow. In this case, the admittance $\bar{\beta}_m$ posesses both real and imaginary parts. As seen in the table, agreement between the exact admittance value and that computed from the finite-element method are good. The wall pressure eigenfunctions for $m = 0$, $m = 1$, and $m = 2$ are plotted in figures 5(a), (b), and (c), respectively. Excellent comparison is again obtained.

A sample calculation for uniform flow, in which $M = 0.2$ and $\tilde{K}_x = 0.5 + 0.5i$ is given in table III. Numerical values of the wall admittance are observed to be in good agreement with the exact values given in the table. The wall pressure eigenfunction, $F(H,z)$, for $m = 0$, $m = 1$, and $m = 2$ were also compared with their exact value. Although the plots are not shown for the sake of brevity, comparisons were consistent with those in figure 5.

The final case involving uniform flow is for a Mach 0.5 flow ($M = 0.5$), with $\tilde{K}_x = 0.5 + 0.5i$. Results for the predicted admittance are tabulated in table IV, and the accuracy is good when compared with the exact values. Wall pressure eigenfunctions for $m = 0$, $m = 1$, and $m = 2$ for this 0.5 Mach number case were plotted and even though results are not shown, trends were identical to those of figure 4.

One-Dimensional Shear

When there is one-dimensional shear so that $\frac{\partial M}{\partial z} = 0$ and $\frac{\partial M}{\partial y} \neq 0$, an exact expression for the admittance is apparently not possible. However, because there is no variation of the mean-flow profile in the z-direction of the tube, numerical results can be compared with those of a one-dimensional analysis presented by Watson (ref. 4). The results which are presented from reference 4 use 1000 points in the y-direction. Further, sample calculations are restricted to a constant gradient sheared flow for which

$$M(y) = \begin{cases} 2M_o \frac{y}{H} & \left(0 \leq y \leq \frac{H}{2}\right) \\ 2M_o \frac{1 - y}{H} & \left(\frac{H}{2} \leq y \leq H\right) \end{cases} \tag{37}$$

where M_o is the centerline Mach number in the tube.

Admittance values for a centerline Mach number of 0.2 ($M_o = 0.2$) and $\tilde{K}_x = 0.5 + 0.5i$ are tabulated in table V. Quantitatively, the eigenvalues computed from the two-dimensional analysis presented in this paper compare well with those obtained by the one-dimensional analysis presented in reference 4. The wall eigenfunctions $F(H,z)$ corresponding to the admittances tabulated in table V have also been computed. Because the mean-flow profile is independent of the coordinate z, the eigenfunction $F(y,z)$ is still defined by equation (30). The wall pressure eigenfunction along the upper wall will be of the form, $\cos m\pi z/L$, just as in the uniform flow case. However, the transverse eigenfunction $F_m(y)$ and wall admittance values β_4 are no longer given by the analytical expressions defined in equations (31) and 33). In fact, $F_m(y)$ must be determined numerically. The wall pressure eigenfunction $F(H,z)$ computed from this analysis are compared with the exact values for $m = 0$, $m = 1$, and $m = 2$ in figures 6(a), (b), and (c), respectively. Values computed from this analysis are indistinguishable from the exact values. Such good comparison between the modes gives further credence to the analysis employed in this paper.

The final sample calculation is for $M = 0.5$ and $\tilde{K}_x = 0.5 + 0.5i$. Admittance calculations are given in table VI. Note that for this reasonably high centerline Mach number, the admittance values computed from this analysis compare well with those computed from reference 4. The wall pressure eigenfunction, $F(H,z)$, for $m = 0$, $m = 1$, and $m = 2$ were consistent with those in figure 6.

Two-Dimensional Shear

Results are now presented for a flow containing gradients in both cross-sectional directions of an impedance tube. In this final example, a demonstration of how data taken from a two-dimensional sheared flow experiment are used in conjunction with the analysis presented here to determine the admittance of a test specimen is given. The experimental data were obtained in the flow impedance test laboratory at the Langley Research Center.

A sketch of the grazing flow impedance tube is shown in figure 7. The tube is 2 inches square, so that $H = L = 2$ inches, and the data were obtained at 2500 hertz. Note that the origin of the coordinate system is chosen in the upper left-hand corner of the tube, so that the test specimen is located on the upper wall when referenced to this origin. Data obtained from the axially transversing microphone establish the attenuation and phase rate characteristics along the length of the test specimen. Attenuation and phase rate data are translated directly into an axial propagation constant (ref. 2).

A plot of sound pressure level (SPL) in decibels as a function of axial distance at 2500 Hz and $M = 0$ is shown in figure 8. The leading and trailing edge of the test specimen is denoted by an asterisk on the X-axis. It is of interest to note that the slope of the curve in figure 8 at axial position x gives the attenuation rate at the position. Further, the curve is linear in regions which are dominated by a single propagating mode. The standing wave patterns in the vicinity of the leading and trailing edge of the specimen indicate the presence of reflections and higher order mode contamination. The analysis presented in this paper is not applicable in these regions because of the presence of multiple modes in the acoustic field. However, the curve is clearly linear for values of x between 27 and 35 centimeters. It is this linear portion of the curve that was used to obtain the attenuation rate. Although the curve is not shown, phase rate data show trends similar to that in figure 8 with the linear portion of the curve covering a much wider range of values of x.

The mean-flow profile in the tube was obtained by aerodynamic measurements, at the 350 points in the cross section. The node points for the finite elements were chosen at points in the domain where mean flow measurements were taken (i.e., $NZ = 9$ and $NY = 34$). Figure 9 gives a graphical representation of the flow profile measured in the tube as a function of the coordinate y, at $z = 1$, $1/2$, and $1/4$ inch. Note that the functional form of the mean-flow profile changes at each of the three z stations so that this profile is not independent of the coordinate z as in the previous section. Further, the centerline Mach number of this profile was determined to be approximately 0.3 ($M_o = 0.3$).

A sample calculation is shown in table VII for no flow, uniform flow, a flow with one-dimensional shear, and the measured flow. The admittance given in the table corresponds to the admittance of the mode which is closest to a plane wave. The flow with one-dimensional shear was constructed by using the profile at $z = L/2$ in fig-

ure 9 (i.e., $M(y,z) = G_3(y)$), whereas the uniform flow value was chosen as the average value of $G_3(y)$ $\left(\text{i.e., } M = \frac{1}{H}\int_0^H G_3(y)\,dy\right)$. Results show that uniform flow calculations agree better with results for one-dimensional shear than the no-flow calculation. Further, the uniform flow profile with the particle displacement continuity (n = 2) as the boundary condition, agrees better with the one-dimensional shear results than the particle velocity boundary condition (n = 1). Note that the uniform flow and one-dimensional sheared flow admittance value differ only moderately from the zero flow value. In contrast the imaginary part of the admittance calculated by using the measured profile, differs significantly from that calculated from the profile with only one-dimensional shear. Such results suggest that for flows over acoustically lined panels, the flow has a significant effect on the acoustic properties of the liner. The reader is reminded however, that this result would be invalidated if the measured value of the wall pressure eigenfunction $F(H,z)$ did not coincide with that calculated from the two-dimensional sheared flow analysis. Unfortunately, measurements of the upper wall eigenfunction were not available and could not be compared with values computed from this analysis.

CONCLUDING REMARKS

A method has been developed for calculating the acoustic admittance of a test specimen located within the wall of a grazing flow impedance tube with flow gradients in both cross-sectional directions. The method, developed and tested for rectangular tubes, may be extended to other geometries as well. In this approach, the unknown admittance value is assumed constant and is obtained by solving an eigenvalue problem. This eigenvalue problem results from the application of the finite-element method to the partial differential equation and boundary conditions governing the acoustic field. A major effort has been devoted toward the solution to this eigenvalue problem, which requires a special scheme to obtain the eigenvalues.

Admittance values determined from the method were compared with exact solutions obtained for a constant mean-flow profile and with results of NASA Technical Paper 2310 for cases involving shear in a single cross-sectional direction. Excellent comparisons were obtained giving credibility to the scheme. Results have been given for the first time in which the flow is represented realistically with gradients in both cross-sectional directions. Limited results obtained for a test specimen installed in the wall of the flow impedance test laboratory at the Langley Research Center suggest that grazing flows can have a significant impact on the acoustic admittance.

NASA Langley Research Center
Hampton, VA 23665-5225
August 23, 1985

REFERENCES

1. Kraft, Robert Eugene: Theory and Measurement of Acoustic Wave Propagation in Multi-Segmented Rectangular Flow Ducts. Ph.D. Diss., Univ. of Cincinnati, 1976.

2. Armstrong, D. L.; Beckemeyer, R. J.; and Olsen, R. F.: Impedance Measurements of Acoustic Duct Liners With Grazing Flow. Boeing paper presented at 87th Meeting of the Acoustical Society of America (New York, New York), Apr. 1974.

3. Mungur, P.; and Gladwell, G. M. L.: Acoustic Wave Propagation in a Sheared Fluid Contained in a Duct. J. Sound & Vib.; vol. 9, no. 1, Jan. 1969, pp. 28-48.

4. Watson, Willie R: A New Method for Determining Acoustic-Liner Admittance in a Rectangular Duct With Grazing Flow From Experimental Data. NASA TP-2310, 1984.

5. Unruh, J. F.; and Eversman, W.: The Transmission of Sound in an Acoustically Treated Rectangular Duct With Boundary Layer. J. Sound & Vib., vol. 25, no. 3, Dec. 1972, pp. 371-382.

6. Desai, Chandrakant S.; and Abel, John F.: Introduction to the Finite Element Method - A Numerical Method for Engineering Analysis. Van Nostrand Reinhold Co., c.1972.

7. Kaufman, Linda: Algorithm 496 - The LZ Algorithm to Solve the Generalized Eigenvalue Problem for Complex Matrices [F2]. ACM Trans. Math. Software, vol. 1, no. 3, Sept. 1975, pp. 271-281.

TABLE I.- ADMITTANCE FOR $M = 0$ AND $\tilde{K}_x = 2.97819i$

m	Exact admittance, $\bar{\beta}_m$	Admittance from finite-element method
0	0.00 + 0.00i	0.00 + 0.00i
1	0.00 + 0.00i	0.00 + 0.00i
2	0.00 - 5.44i	0.00 - 5.45i
3	0.00 - 8.89i	0.00 - 8.98i
4	0.00 - 12.17i	0.00 - 12.23i
5	0.00 - 15.39i	0.00 - 15.52i

TABLE II.- ADMITTANCE FOR $M = 0$ AND $\tilde{K}_x = 0.5 + 0.5i$

m	Exact admittance, $\bar{\beta}_m$	Admittance from finite-element method
0	1.13 + 1.21i	1.13 + 1.21i
1	0.09 - 2.97i	0.09 - 2.97i
2	0.04 - 6.20i	0.04 - 6.21i
3	0.03 - 9.37i	0.03 - 9.40i
4	0.02 - 12.53i	0.02 - 12.59i
5	0.02 - 15.68i	0.02 - 15.81i

TABLE III.- ADMITTANCE FOR $M = 0.2$ AND $\tilde{K}_x = 0.5 + 0.5i$

m	Exact admittance, $\bar{\beta}_m$	Admittance from finite-element method
0	1.20 + 0.90i	1.20 + 0.90i
1	0.49 - 3.28i	0.49 - 3.28i
2	0.82 - 6.82i	0.82 - 6.83i
3	1.18 - 10.29i	1.19 - 10.32i
4	1.56 - 13.95i	1.57 - 13.83i
5	1.94 - 17.21i	1.95 - 17.35i

TABLE IV.- ADMITTANCE FOR $M = 0.5$ AND $\tilde{K}_x = 0.5 + 0.5i$

m	Exact admittance, $\bar{\beta}_m$	Admittance from finite-element method
0	1.25 + 0.66i	1.25 + 0.66i
1	1.40 - 3.60i	1.40 - 3.60i
2	2.58 - 7.46i	2.58 - 7.47i
3	3.82 - 11.26i	3.83 - 11.29i
4	5.06 - 15.04i	5.09 - 15.12i
5	6.31 - 18.82i	6.36 - 18.97i

TABLE V.- ADMITTANCE FOR $M_o = 0.2$, $\tilde{K}_x = 0.5 + 0.5i$, AND CONSTANT GRADIENT ONE-DIMENSIONAL SHEARED FLOW

m	Admittance from one-dimensional analysis (ref. 5)	Admittance from present analysis
0	1.19 + 1.17i	1.12 + 1.20i
1	0.30 - 3.2i	0.31 - 3.17i
2	0.26 - 6.41i	0.27 - 6.43i
3	0.24 - 9.59i	0.26 - 9.63i
4	0.23 - 12.76i	0.26 - 12.82i
5	0.22 - 15.94i	0.25 - 16.00i

TABLE VI.- ADMITTANCE FOR $M_o = 0.5$, $\tilde{K}_x = 0.5 + 0.5i$, AND CONSTANT GRADIENT ONE-DIMENSIONAL SHEARED FLOW

m	Admittance from one-dimensional analysis (ref. 5)	Admittance from present analysis
0	1.27 + 1.22i	1.29 + 1.31i
1	0.71 - 3.42i	0.74 - 3.44i
2	0.63 - 6.71i	0.68 - 6.76i
3	0.58 - 9.88i	0.64 - 9.96i
4	0.56 - 13.06i	0.63 - 13.17i
5	0.55 - 16.24i	0.62 - 16.39i

TABLE VII.- ADMITTANCE CALCULATED FOR TEST SAMPLE AT MACH NUMBER OF 0.3

Flow profile	Admittance
No flow $\tilde{K}_x = 1.12 - 0.25i$	0.54 + 0.610i
Uniform flow $\tilde{K}_x = 0.89 - 0.14i$	
n = 1	0.49 + 0.550i
n = 2	0.67 + 0.690i
One-dimensional flow $\tilde{K}_x = 0.89 - 0.14i$	0.61 + 0.583i
Measured $\tilde{K}_x = 0.89 - 0.14i$	0.60 + 0.150i

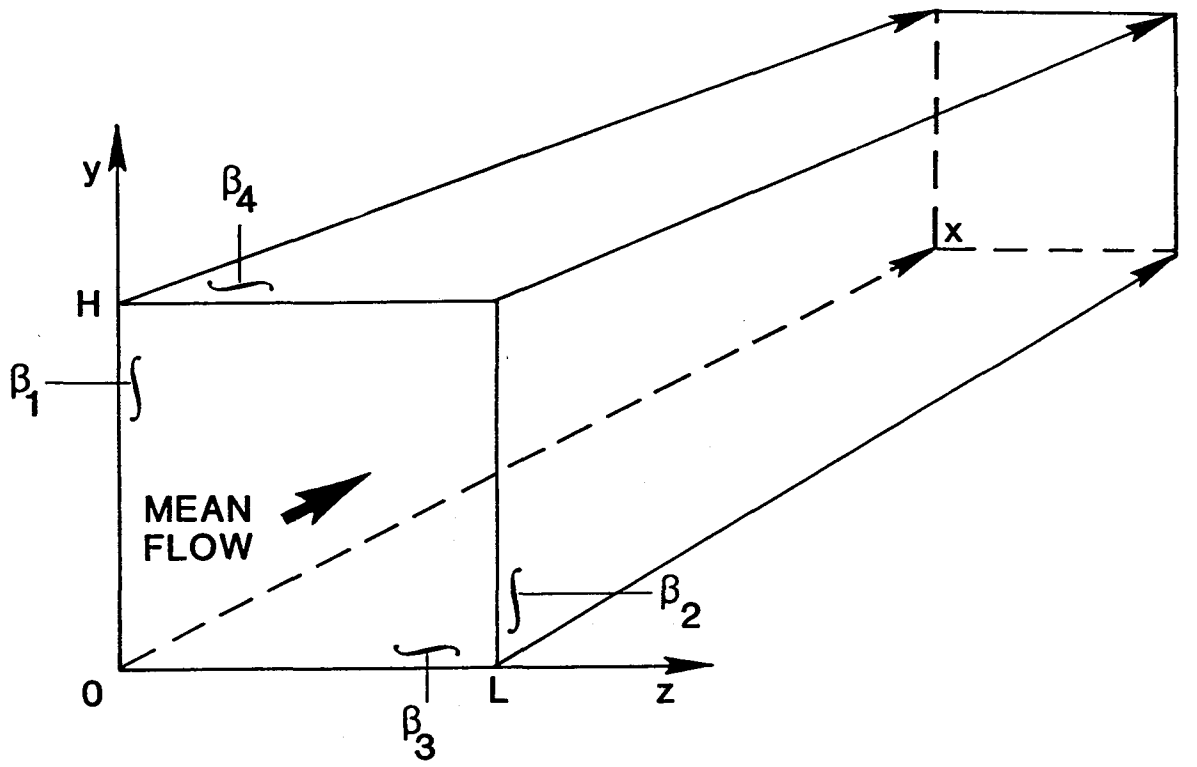

Figure 1.- Grazing flow impedance tube and coordinate system.

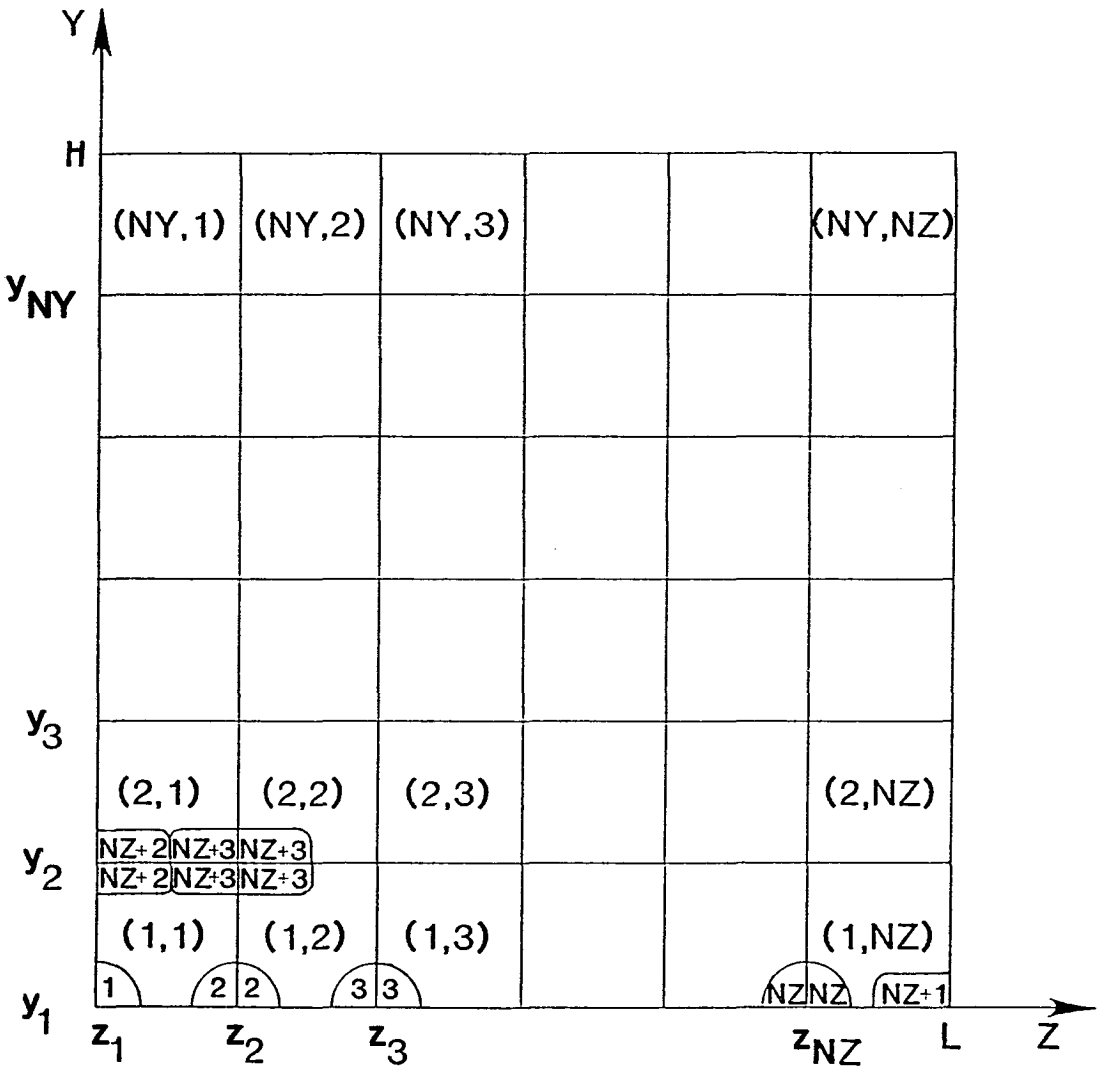

Figure 2.- Finite-element discretization.

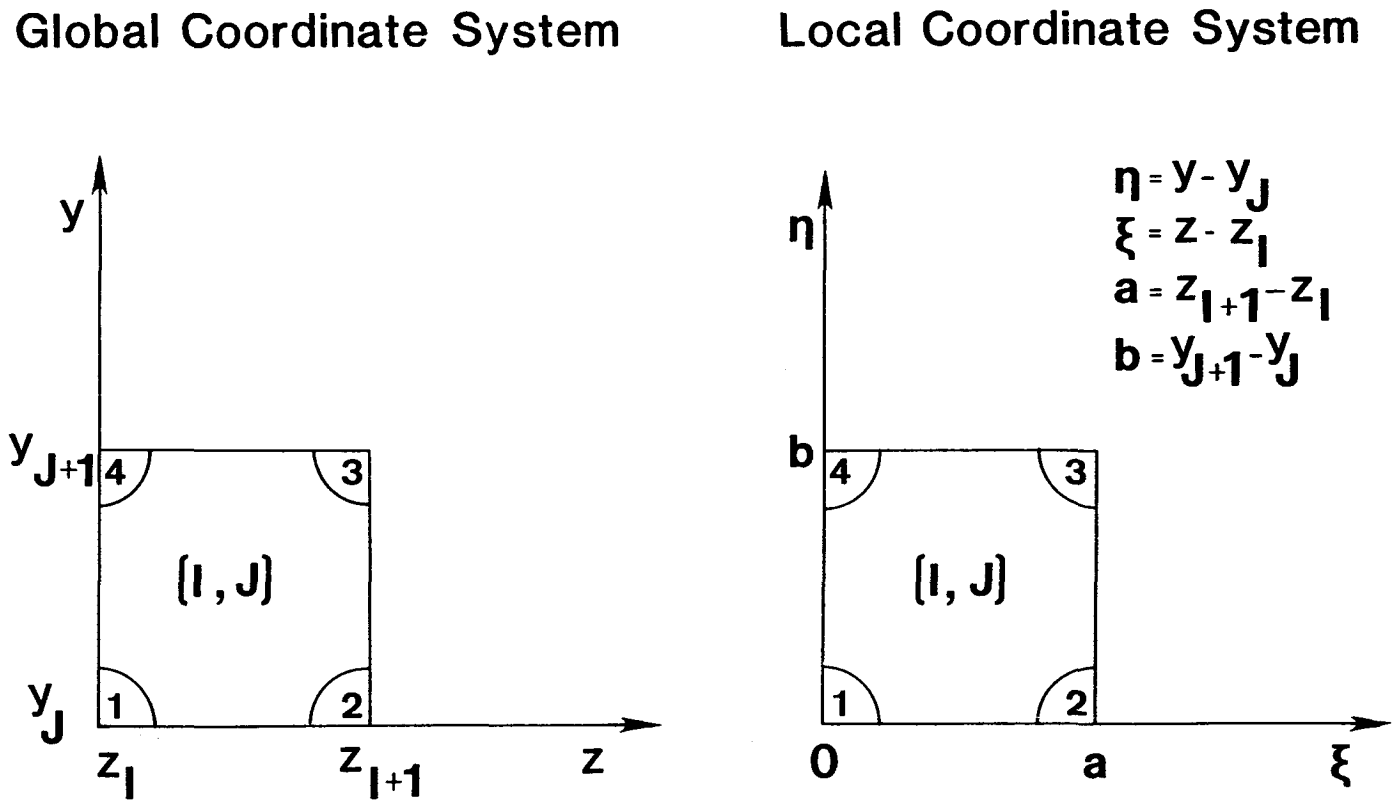

Figure 3.- Global and local coordinate system for a typical finite element.

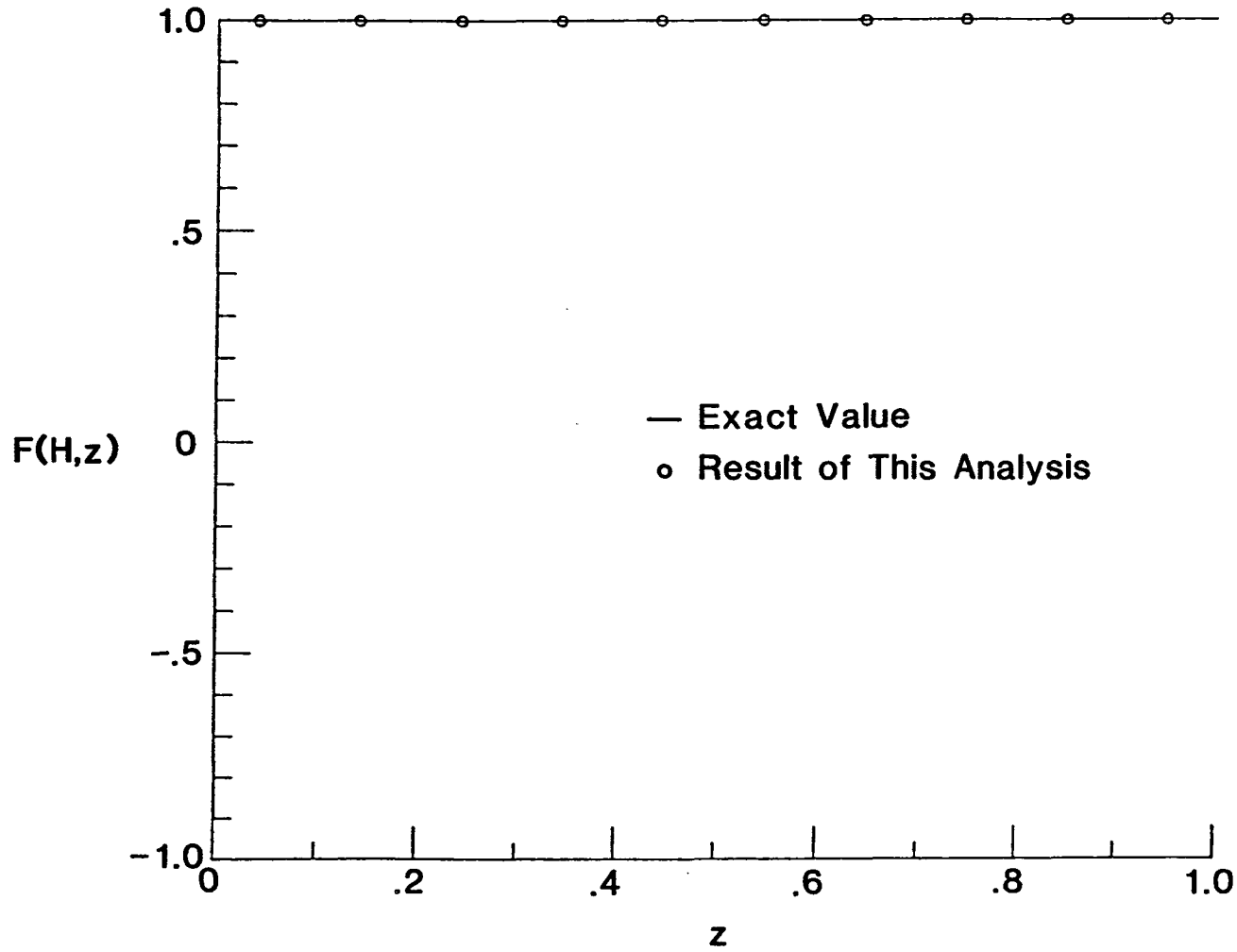

(a) m = 0.

Figure 4.- Wall pressure eigenfunctions for $\tilde{K}_x$ = 2.97819i and M = 0.

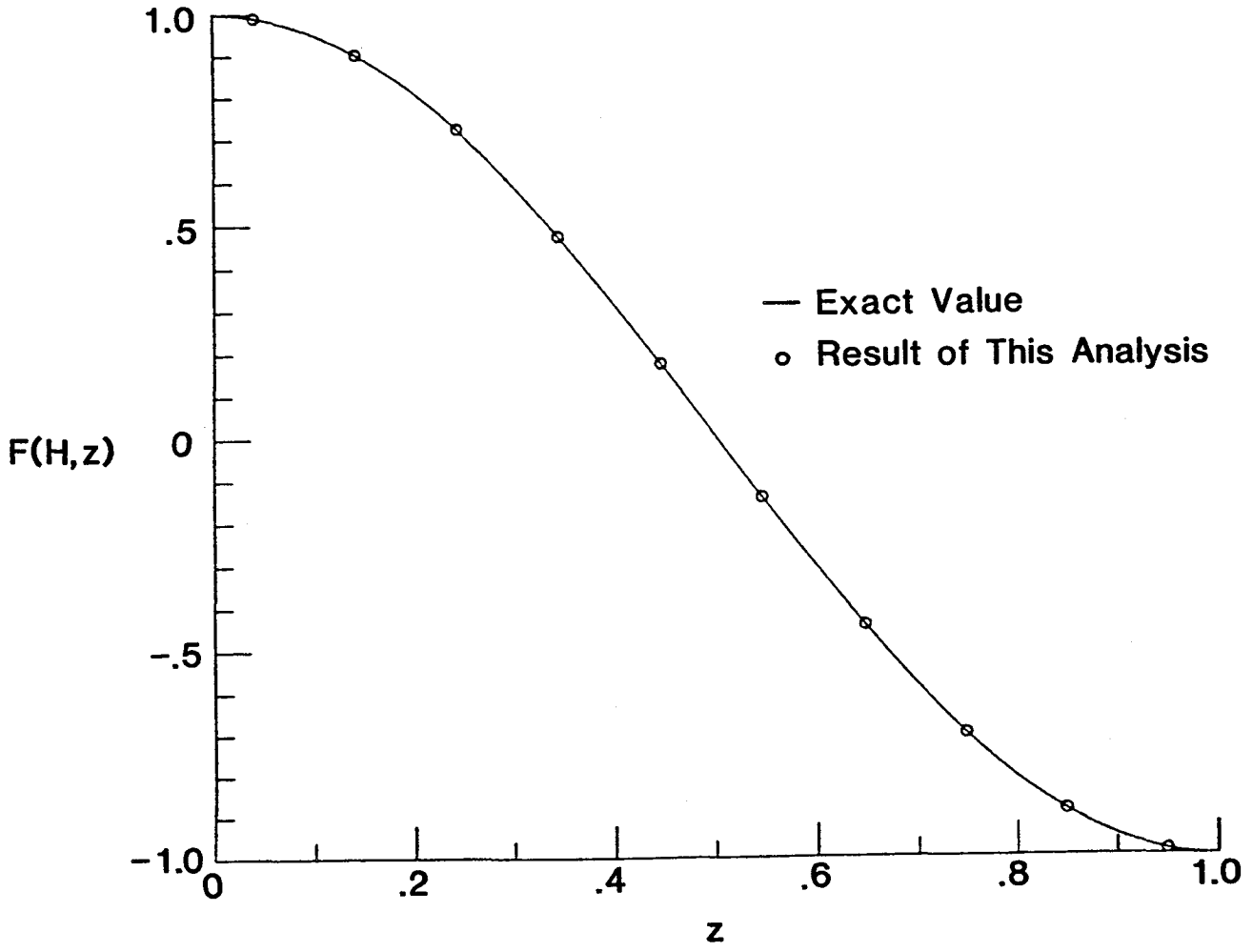

(b) m = 1.

Figure 4.- Continued.

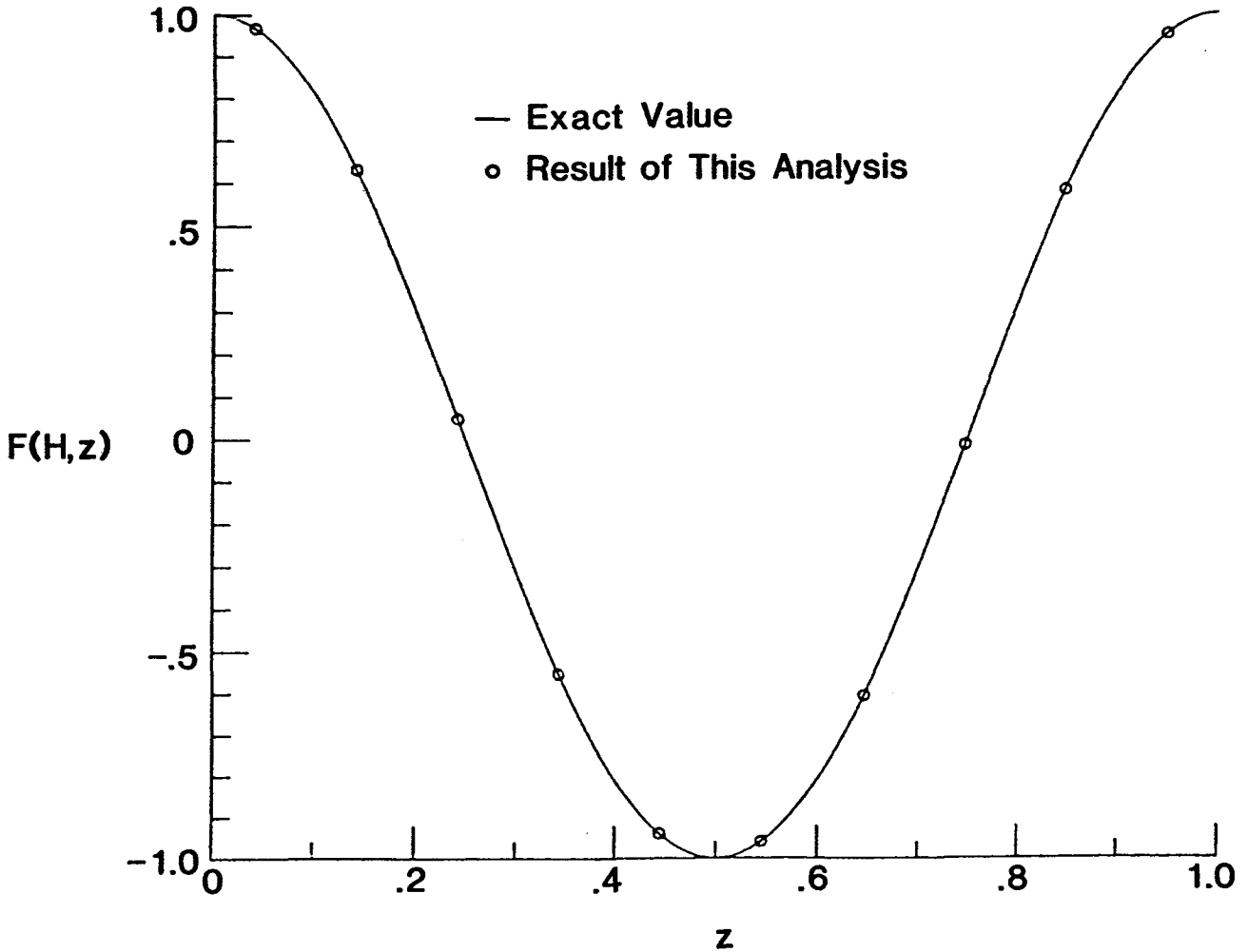

(c) m = 2.

Figure 4.- Concluded.

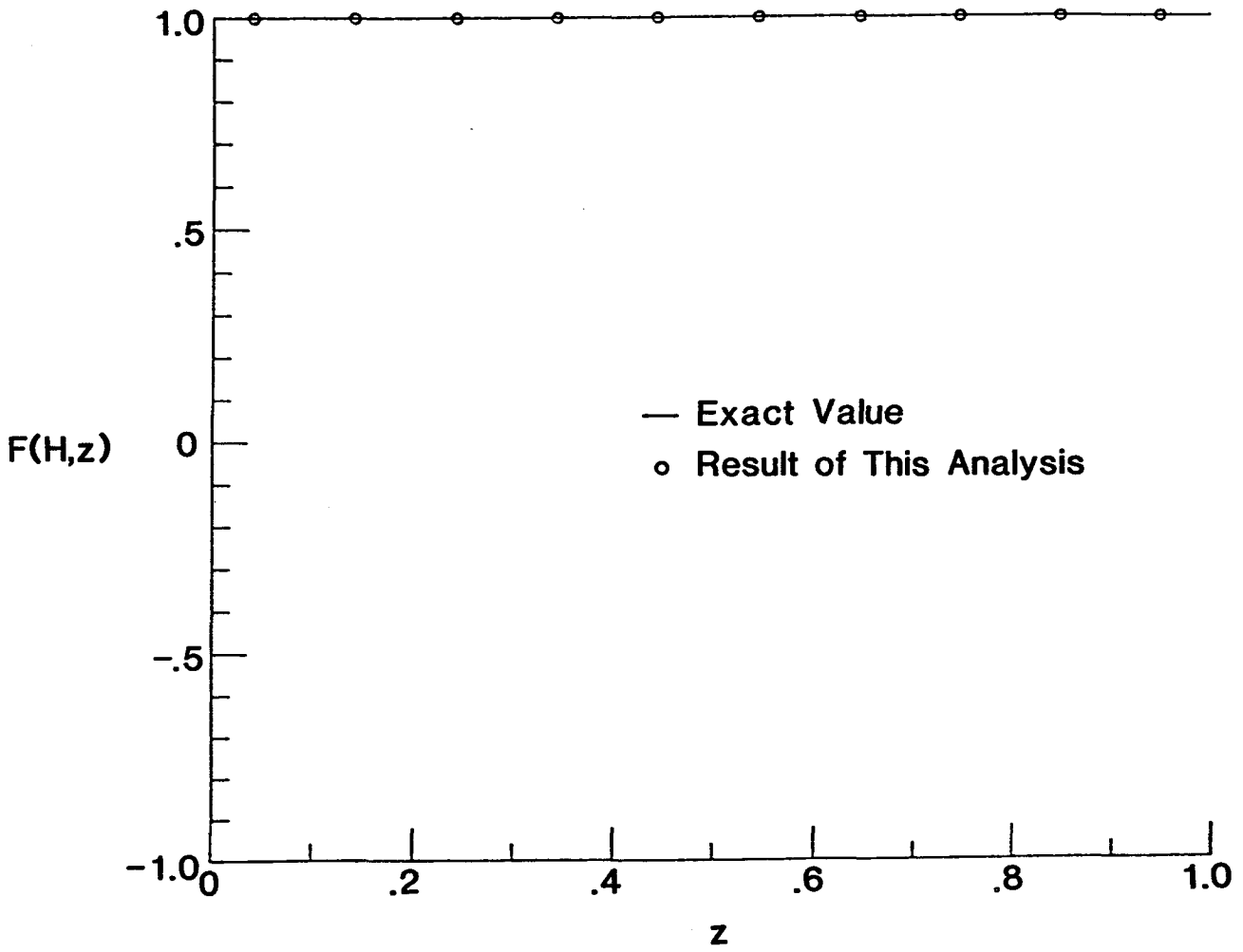

(a) m = 0.

Figure 5.- Wall pressure eigenfunctions for $\tilde{K}_x = 0.5 + 0.5i$ and M = 0.

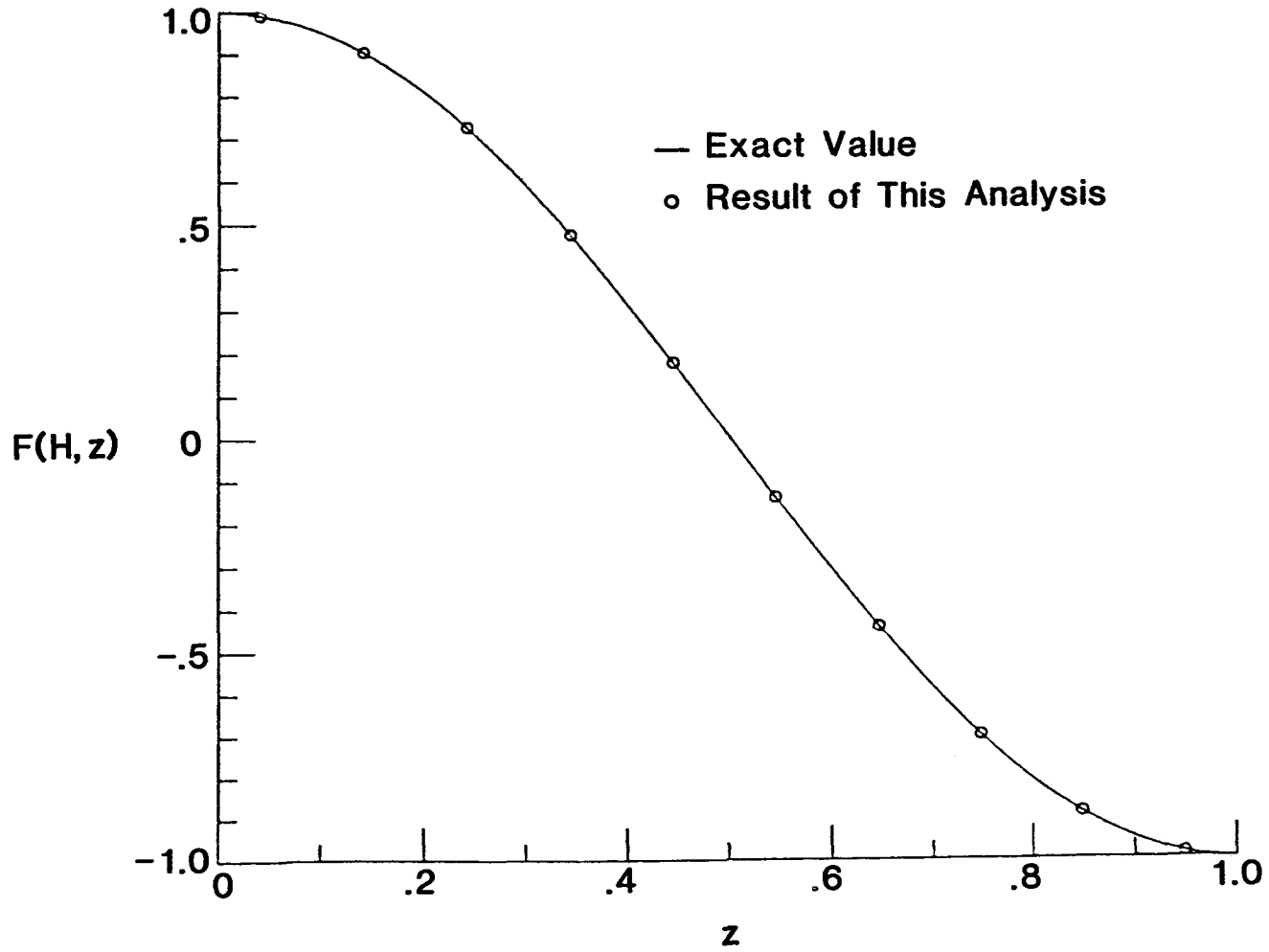

(b) m = 1.

Figure 5.- Continued.

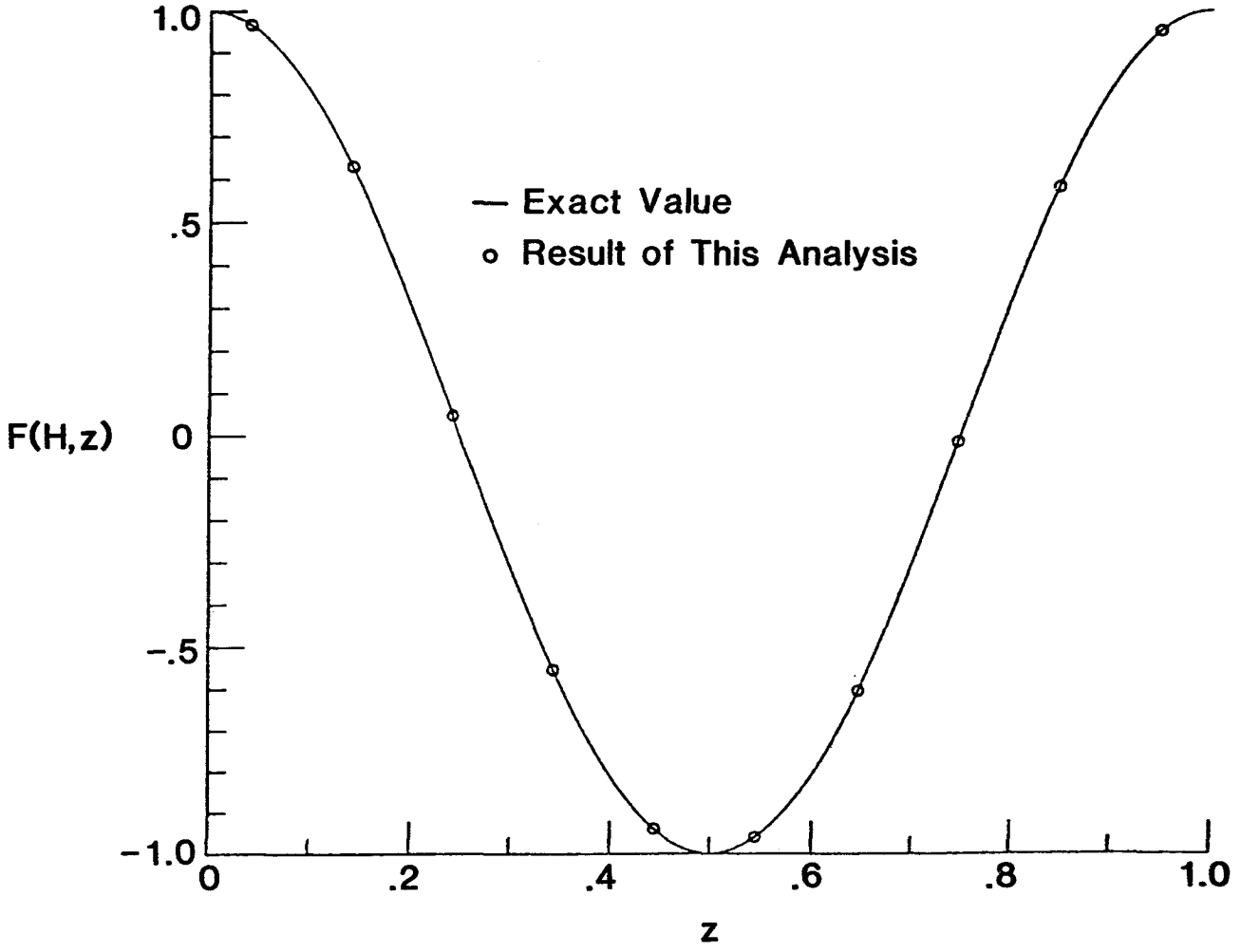

(c) m = 2.

Figure 5.- Concluded.

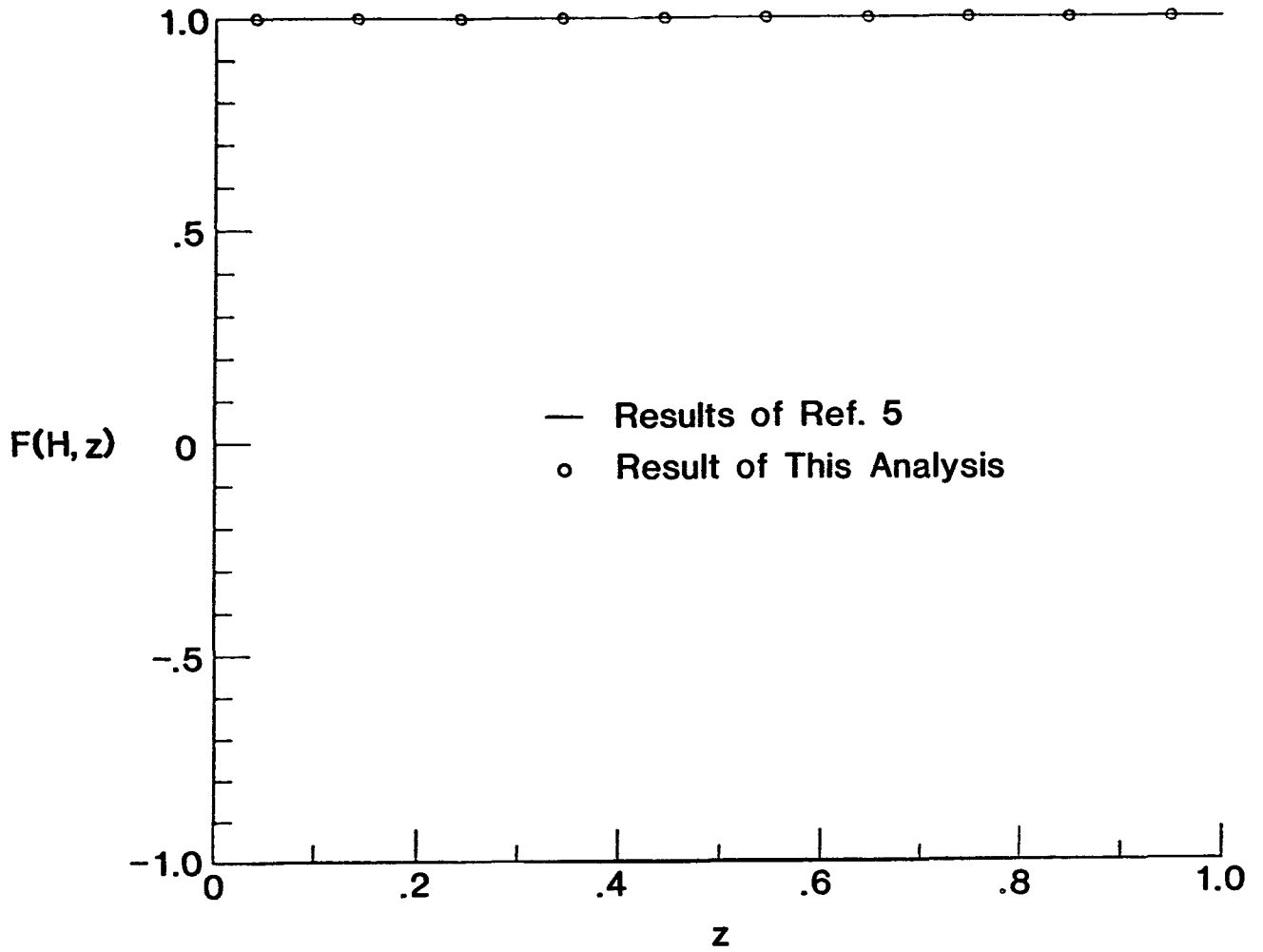

(a) m = 0.

Figure 6.- Wall pressure eigenfunctions for one-dimensional sheared flow, $\tilde{K}_x = 0.5 + 0.5i$ and $M_o = 0.2$.

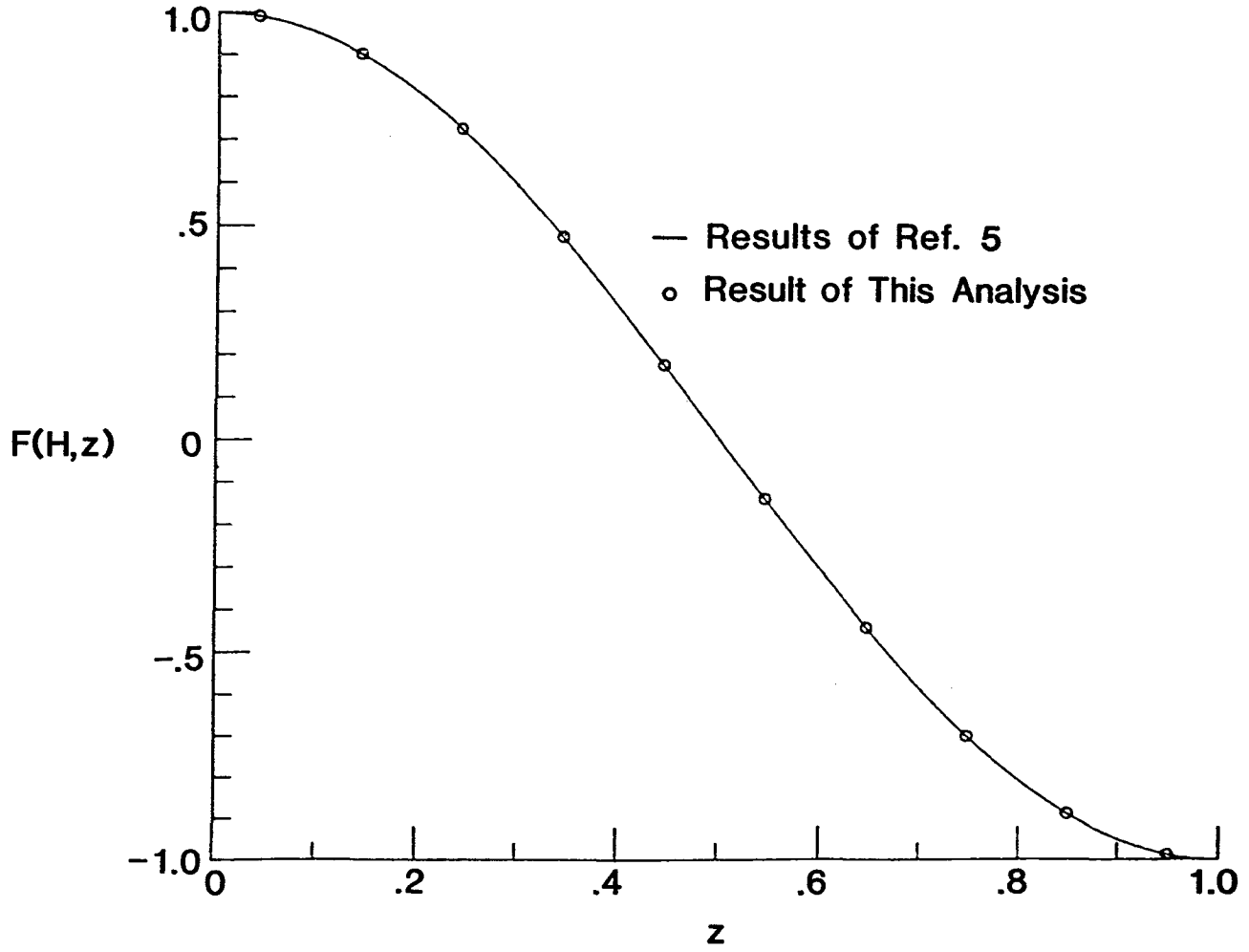

(b) m = 1.

Figure 6.- Continued.

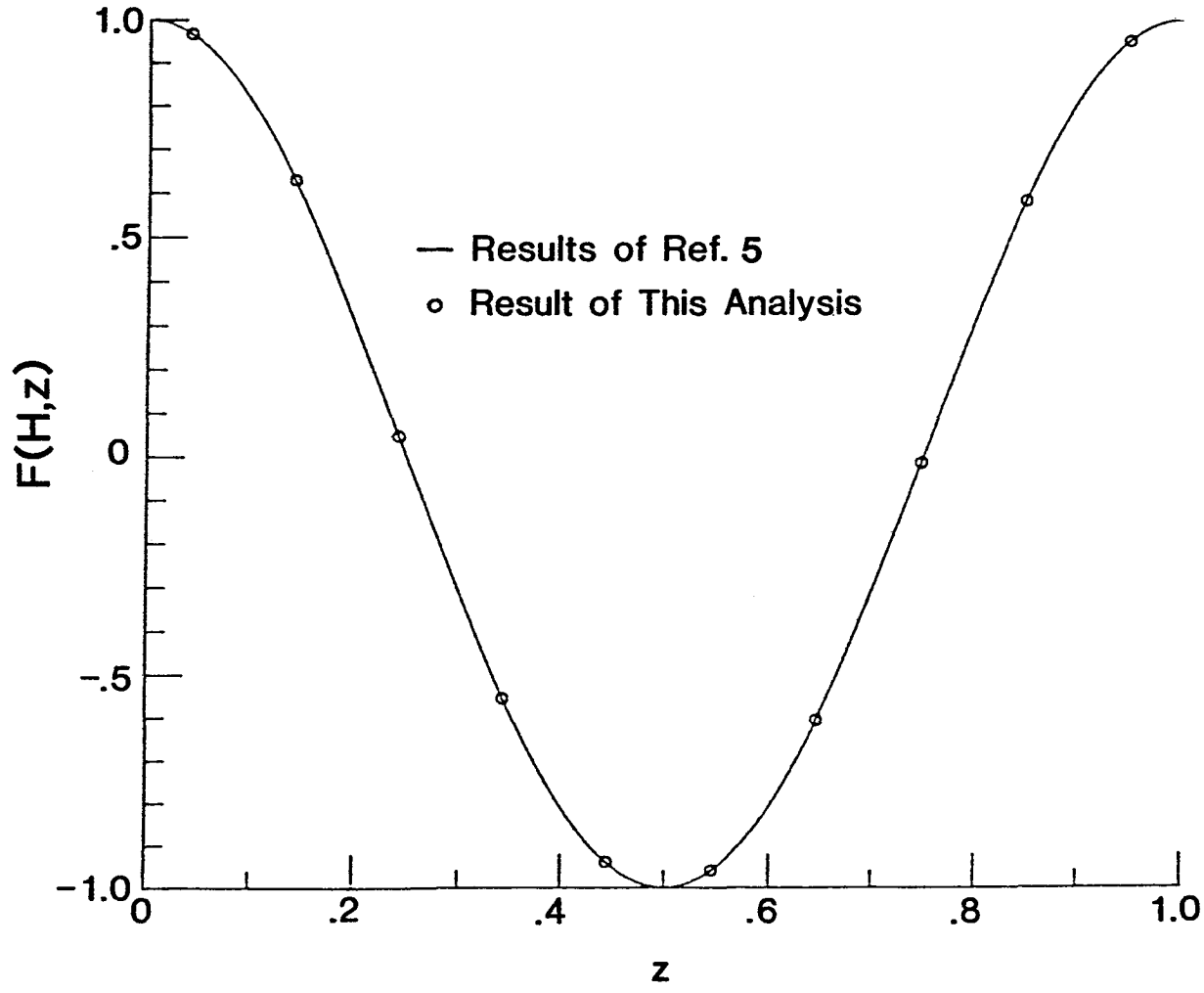

(c) m = 2.

Figure 6.- Concluded.

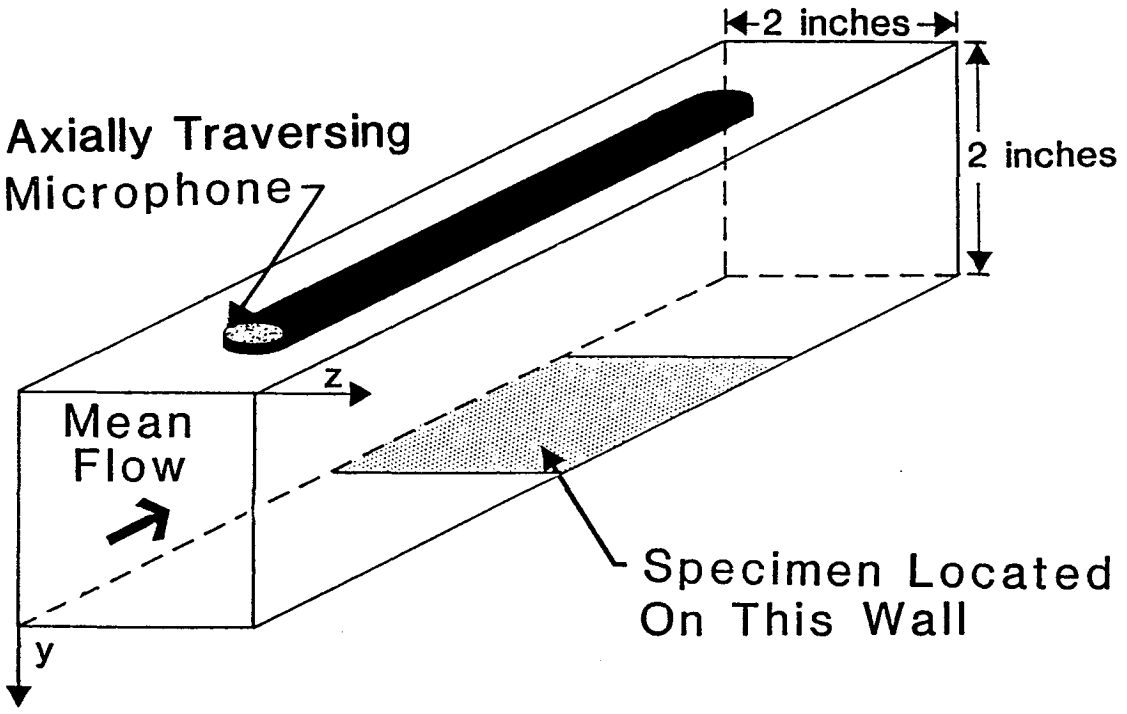

Figure 7.- Schematic of grazing flow impedance tube facility.

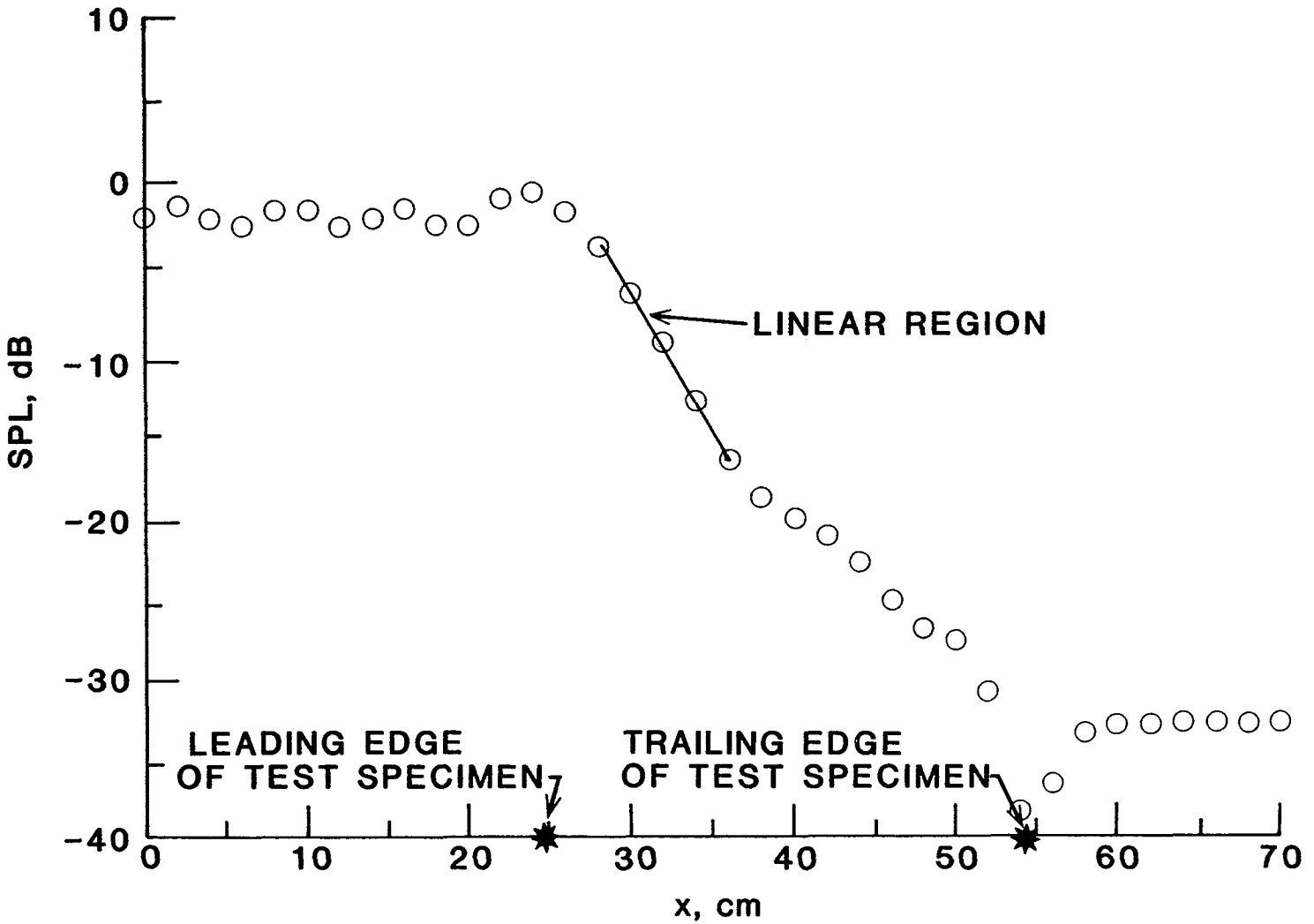

Figure 8.- Decrease in sound pressure level as a function of axial location. 2500 Hz; M = 0.

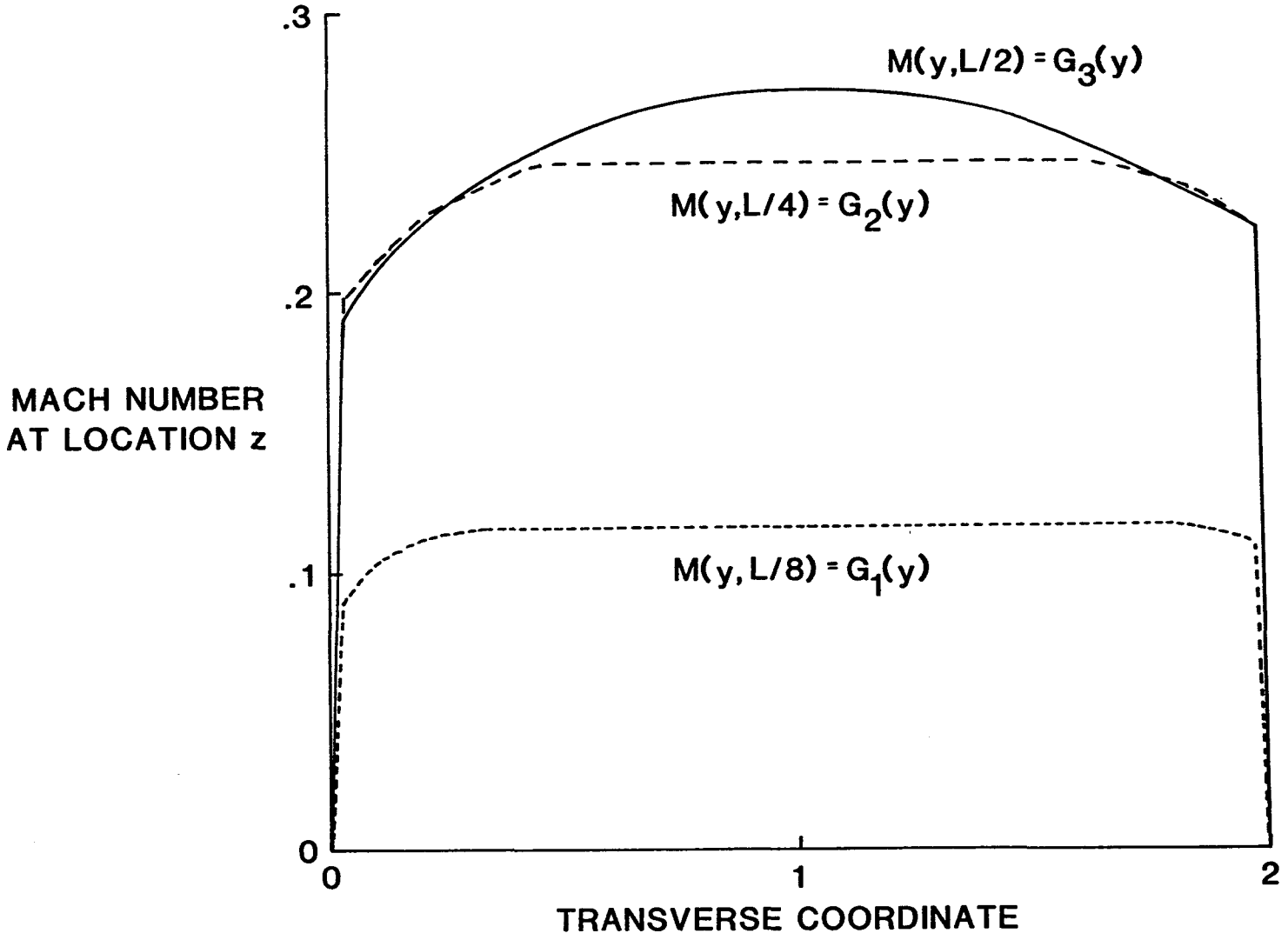

Figure 9.- Measured Mach number profiles at three different z-locations.
L = 2 in.

1. Report No.	2. Government Accession No.	3. Recipient's Catalog No.
NASA TP-2518		

4. Title and Subtitle	5. Report Date
A Method for Determining Acoustic-Liner Admittance in Ducts With Sheared Flow in Two Cross-Sectional Directions	October 1985
	6. Performing Organization Code 505-31-33-13
7. Author(s) Willie R. Watson	8. Performing Organization Report No. L-15997
	10. Work Unit No.
9. Performing Organization Name and Address NASA Langley Research Center Hampton, VA 23665-5225	11. Contract or Grant No.
	13. Type of Report and Period Covered Technical Paper
12. Sponsoring Agency Name and Address National Aeronautics and Space Administration Washington, DC 20546-0001	14. Sponsoring Agency Code

15. Supplementary Notes

16. Abstract

A method is developed for determining the acoustic admittance of a test liner installed in the wall of a grazing flow impedance tube. The mean flow is permitted flow gradients in both cross-sectional directions of the tube. The unknown admittance value is obtained by solving an eigenvalue problem. This eigenvalue problem results from the application of the finite-element method to the partial differential equation and boundary conditions governing the acoustic field. The credibility of the method is established by comparing results with exact solutions obtained for a constant mean-flow profile and with previous results for cases involving shear in only one cross-sectional direction. Excellent comparisons were obtained in both cases. The analysis has been used in conjunction with a limited amount of experimental data and shows that the flow must be accurately modeled in order to determine the acoustic-liner properties.

17. Key Words (Suggested by Author(s))	18. Distribution Statement
Duct acoustics Acoustic impedance Suppression Sound-absorbing materials	Unclassified - Unlimited Subject Category 71

19. Security Classif. (of this report)	20. Security Classif. (of this page)	21. No. of Pages	22. Price
Unclassified	Unclassified	37	A03

N-305 For sale by the National Technical Information Service, Springfield, Virginia 22161

NASA